

UHI Research Database pdf download summary

Metabolism in anoxic permeable sediments is dominated by eukaryotic dark fermentation

Bourke, Michael F.; Marriott, Philip J; Glud, Ronnie N.; Hasler-Sheetal, Harald; Kamalanathan, Manoj; Beardall, John; Chris, Greening; Cook, Perran L.M:

Published in:
Nature Geoscience

Publication date:
2016

Publisher rights:
© 2016 Springer Nature Limited. All rights reserved.

The re-use license for this item is:
CC BY-NC-ND

The Document Version you have downloaded here is:
Early version, also known as pre-print

The final published version is available direct from the publisher website at:
[10.1038/ngeo2843](https://doi.org/10.1038/ngeo2843)

[Link to author version on UHI Research Database](#)

Citation for published version (APA):

Bourke, M. F., Marriott, P. J., Glud, R. N., Hasler-Sheetal, H., Kamalanathan, M., Beardall, J., Chris, G., & Cook, P. L. M. (2016). Metabolism in anoxic permeable sediments is dominated by eukaryotic dark fermentation. *Nature Geoscience*, 10(1), 30-35. <https://doi.org/10.1038/ngeo2843>

General rights

Copyright and moral rights for the publications made accessible in the UHI Research Database are retained by the authors and/or other copyright owners and it is a condition of accessing publications that users recognise and abide by the legal requirements associated with these rights:

- 1) Users may download and print one copy of any publication from the UHI Research Database for the purpose of private study or research.
- 2) You may not further distribute the material or use it for any profit-making activity or commercial gain
- 3) You may freely distribute the URL identifying the publication in the UHI Research Database

Take down policy

If you believe that this document breaches copyright please contact us at RO@uhi.ac.uk providing details; we will remove access to the work immediately and investigate your claim.

Published in final edited form as:

Nat Geosci. 2017 January ; 10(1): 30–35. doi:10.1038/ngeo2843.

Metabolism in anoxic permeable sediments is dominated by eukaryotic dark fermentation

Michael F Bourke^{a,*}, Philip J. Marriott^b, Ronnie N. Glud^{c,e,f}, Harald Hasler-Sheetal^{c,d}, Manoj Kamalanathan^g, John Beardall^h, Chris Greening^h, and Perran L.M. Cook^{a,*}

^aWater Studies Centre, School of Chemistry, Monash University, Wellington Road, Clayton, VIC 3800, Australia

^bAustralian Centre for Research on Separation Science, School of Chemistry, Monash University, Wellington Road, VIC 3800, Australia

^cUniversity of Southern Denmark, Nordic Centre for Earth Evolution, Odense M-5230, Denmark

^dUniversity of Southern Denmark, Villum Center for Bioanalytical Sciences, Odense M-5230, Denmark

^eScottish Association for Marine Science, Oban PA37 1QA, UK

^fUniversity of Aarhus, Arctic Research Centre, Aarhus, Denmark

^gDepartment of Marine Biology, Texas A&M University. Galveston, TX, 77554 USA

^hSchool of Biological Sciences, Monash University, Clayton, VIC 3800, Australia

Abstract

Permeable sediments are common across continental shelves and are critical contributors to marine biogeochemical cycling. Organic matter in permeable sediments is dominated by microalgae, which as eukaryotes have different anaerobic metabolic pathways to prokaryotes such as bacteria and archaea. Here we present analyses of flow-through reactor experiments showing that dissolved inorganic carbon is produced predominantly as a result of anaerobic eukaryotic metabolic activity. In our experiments, anaerobic production of dissolved inorganic carbon was consistently accompanied by large dissolved H₂ production rates, suggesting the presence of fermentation. The production of both dissolved inorganic carbon and H₂ persisted following administration of broad spectrum bactericidal antibiotics, but ceased following treatment with metronidazole. Metronidazole inhibits the ferredoxin/hydrogenase pathway of fermentative eukaryotic H₂ production, suggesting that pathway as the source of H₂ and dissolved inorganic carbon production. Metabolomic analysis showed large increases in lipid production at the onset of anoxia, consistent with documented pathways of anoxic dark fermentation in microalgae. Cell

Users may view, print, copy, and download text and data-mine the content in such documents, for the purposes of academic research, subject always to the full Conditions of use:http://www.nature.com/authors/editorial_policies/license.html#terms

*Correspondence may be directed to PLMC or MFB, using perran.cook@monash.edu or michael.bourke@monash.edu, respectively.

Author contributions

All FTR experiments were performed by MFB and supervised by PLMC. MFB and PLMC were responsible for experimental design and research direction with significant input from RNG and JB. Effluent volatile fatty acid analysis was performed by MFB and supervised by PJM. Metabolomics analysis was performed by HHS. Algal culture experiments were performed by MK and MFB and supervised by JB and PLMC. Manuscript was written by MFB and PLMC. All authors contributed to discussion and editing.

counts revealed a predominance of microalgae in the sediments. H₂ production was observed in dark anoxic cultures of diatoms (*Fragilariopsis* sp.) and a chlorophyte (*Pyramimonas*) isolated from the study site, substantiating the hypothesis that microalgae undertake fermentation. We conclude that microalgal dark fermentation could be an important energy-conserving pathway in permeable sediments.

Keywords

H₂ production; Dark fermentation; Diatom; Sand

Permeable sediments and organic matter metabolism

Microalgae are globally ubiquitous in photic sediments and often have a biomass exceeding phytoplankton in overlying waters¹. In permeable (sandy) sediments, their biomass may comprise 10 – 40% of the organic carbon pool based on previously reported carbon to chlorophyll *a* ratios^{2,3} and a high proportion of functional chlorophyll⁴. In contrast, bacterial biomass has previously been reported to comprise <10% of the organic carbon pool in sandy sediments⁵. This is also consistent with the dominance of microalgae in mediating carbon flows in such sediments⁶. Given their high biomass, it is reasonable to expect that microalgae will undertake a large fraction of the carbon mineralization and energy generation pathways in comparison to bacteria. Despite this, it remains widely assumed that bacterial fermentation and sulfate reduction are the main mechanisms of dissolved inorganic carbon (DIC) production in anoxic permeable sediments⁷. Surprisingly, there have been no systematic studies of electron acceptor utilisation in freshly collected sands and, despite their dominance, the role of microalgae in these processes⁸.

The dynamic nature of permeable sediments means that microalgae are often observed to be evenly distributed to 15 cm within sands where dark anoxic conditions will prevail^{1,6}. It has been shown that microalgae mixed into the dark sediment can remain viable for long periods of time (half-lives of 6-22 days), highlighting their adaptation to this dynamic environment⁹. However, the metabolic basis of how they survive light and oxygen fluctuations is unclear. Nitrate respiration has previously been shown to sustain the survival of axenic cultures of phototrophic eukaryotes in dark anoxic conditions¹⁰; however, it remains to be determined whether nitrate respiration is a relevant strategy in the environment and it is unlikely that it is sufficient to support microalgal populations in oligotrophic systems with low nitrate concentrations. Fermentation is an alternative strategy that microorganisms use to couple carbon mineralization to energy-generation. While some microalgae have been shown to undertake fermentation under dark anoxic conditions, for example chlorophytes^{11,12}, there have been no studies to date to quantify the importance of this in the environment.

In this work, we present the first study of the importance of anoxic microalgal metabolism in permeable sediments. We combined flow through reactor experiments with microbiological approaches to determine the dominant contributors and pathways of dissolved inorganic carbon (DIC) production in permeable sediments. We show that microalgal dark

fermentation is the dominant metabolic pathway, which is the first time this has been documented in an environmental setting.

Phototrophic eukaryotes dominate metabolism

We initially compared the rates of DIC production and electron acceptor utilization using sediments collected at Port Philip Bay (Australia) and Kerteminde (Denmark). We used flow through reactors (FTRs) to compare solute concentrations at the inlet and outlet of a sand column in order to calculate volumetric rates. Under anoxic conditions with the addition of $50 \mu\text{M } ^{15}\text{NO}_3^-$, the FTR experiments showed that rates of nitrate reduction to nitrite and N_2 were low compared to DIC production; they were only able to account for less than 10% of DIC production in Australian and Danish samples (Fig 1a & 1b). This gap between the rate of DIC production and nitrate reduction is consistent with previous observations by Evrard *et al* 2013¹³ and Marchant *et al* 2016¹⁴, suggesting a common, although not ubiquitous¹⁵, phenomenon. Rates of iron (II), sulfide and methane production in the presence of nitrate were less than 0.6 , 0.2 and $0.05 \text{ nmol mL}^{-1} \text{ h}^{-1}$, respectively, which cannot account for the DIC production rates observed. We rule out significant rates of iron reduction and subsequent trapping of Fe^{2+} as FeS or sorption onto FeOOH on the basis that no alkalinity production ($<10 \text{ nmol mL}^{-1} \text{ h}^{-1}$) was observed and also the low reactive iron pool present in permeable sediments¹⁶. Likewise, measurements of intracellular nitrate were negligible ($<1.5 \text{ nmol mL}^{-1}$), ruling out the use of an accumulated intracellular nitrate pool by diatoms¹⁷. We also dismiss abiotic processes such as carbonate dissolution driving DIC production given the absence of alkalinity production. There was no significant difference in DIC production between oxic and anoxic conditions ($p = 0.76$) and in the presence or absence of nitrate (ANOVA, two factor with replication, $p = 0.44$) (Fig 1c); this suggests that the organisms responsible for DIC production under oxic conditions were able to use an energy-conservation pathway to maintain their metabolism under anoxia, and that nitrate, iron or sulfate reduction were not significantly contributing to this, consistent with Figures 1a and 1b.

To elucidate which group of organisms were involved in the DIC production under anoxic conditions, FTRs containing the Australian sediments were exposed to three seawater reservoir treatments: a control treatment, one spiked with 50 mg L^{-1} of amoxicillin, and one spiked with $2 \text{ mmol L}^{-1} \text{ HgCl}_2$. The production of DIC was shown to be halted by the mercuric chloride treatment (Fig 1d), indicating that carbon mineralization was driven by biotic processes. However, there was no significant difference between the DIC production rates of the control and amoxicillin treatments (ANOVA, single factor, $p = 0.80$), indicating that amoxicillin did not inhibit the dominant microbial community responsible for carbon mineralization. Amoxicillin is a broad spectrum antibiotic that has been shown to exhibit bactericidal action at concentrations in the range of 0.1 to 2 mg L^{-1} depending on the strain of bacteria¹⁸. If bacteria were responsible for producing DIC, we would expect to see a decrease in the DIC production rate in the amoxicillin treatment compared to the control. This suggests that eukaryotes, not bacteria, are responsible for the vast majority of DIC production in permeable sediments. The possibility of bacteria being resistant to amoxicillin was investigated by quantifying the rate of denitrification (primarily a bacterial process) in the presence and absence of amoxicillin (see Supplementary Information Figure S1). As

expected, amoxicillin inhibited denitrification by factors of 2 to 5, compared to the control, over the course of the experiment, suggesting that antibiotic resistant bacteria do not explain our observations.

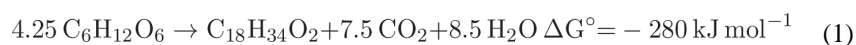
Possible eukaryotic organisms responsible for DIC production include meiofauna, macrofauna and microalgae. We ruled out macrofauna and meiofauna on the basis that DIC production was maintained for over 10 days after anoxia (data not shown), which would kill these organisms, and that no macrofauna were observed in the sediment. We therefore hypothesized that the source of the DIC production is microalgae, such as diatoms, chlorophytes, and other eukaryotic microalgae. Consistent with this, cell counting revealed a diverse community of microalgae at the study site (see Supplementary Information, Table S2). Diatoms were particularly abundant, exceeding 10^5 cells per mL, with species from the genus *Amphora*, *Cocconeis*, and *Fragilariopsis* most numerous. Scaling the sediment chlorophyll *a* content to total microalgae using a carbon to chlorophyll *a* ratio of 40^3 gives a sediment microphytobenthos carbon content of 850-860 $\mu\text{g g}^{-1}$ of dry sediment, which comprises approximately 57% of the total organic content of the sediment, highlighting the likely dominance of these organisms in DIC production.

Eukaryotic dark fermentation pathways are the major source of DIC production under anoxic conditions

Having demonstrated that the major respiratory electron acceptors in marine systems cannot account for DIC production, we looked for other potential sources that may be responsible for carbon mineralization. Intriguingly, we observed through microsensors experiments that H_2 production began ~36 hours after the commencement of anoxia. H_2 concentrations in the FTR reached $44 \pm 10 \mu\text{mol L}^{-1}$ and $23 \pm 4 \mu\text{mol L}^{-1}$ (data not shown) in the presence and absence of nitrate, respectively (Figure 2a). These concentrations are almost an order of magnitude higher than previously reported maximum transient concentrations of H_2 by bacterial fermentation of 2 to 6 μM ^{19,20}. These values correspond to production rates of $26 \pm 7 \text{ nmol mL}^{-1} \text{ h}^{-1}$ and $13 \pm 2 \text{ nmol mL}^{-1} \text{ h}^{-1}$ whereas DIC production rates in these columns were 81 ± 36 and $117 \pm 46 \text{ nmol mL}^{-1} \text{ h}^{-1}$ for anoxic treatments with and without nitrate, respectively (data not shown). The addition of the antibiotic ciprofloxacin at a concentration of $150 \mu\text{mol L}^{-1}$ to the columns had no effect on H_2 production (Figure 2a). Single species assays have shown ciprofloxacin to have an EC-50 value of between 15 and 51 nmol L^{-1} for typical gram positive bacteria^{21,22}, and 241 nmol L^{-1} for the gram negative bacteria of *Pseudomonas putida*²³. Eukaryotes have been shown to be far less sensitive to ciprofloxacin, as the EC-50 values for green algal species *Selenastrum capricornutum* and *Pseudokirchneriella subcapitata* range between 9000 nmol L^{-1} and 56,000 nmol L^{-1} ²⁴. Despite the presence of ciprofloxacin, H_2 production persisted in both control and nitrate treatments, and indeed continued to increase over the course of the experiment. This strongly suggests that, as with DIC production, H_2 production cannot be attributed to a bacterial source and is therefore likely being produced by eukaryotes which are known to be capable of H_2 production through fermentation under anoxia²⁵.

There are two well-studied eukaryotic metabolic processes that produce H₂: photobiological production and dark fermentative metabolism²⁵. In photobiological production, light-excited electrons derived from water (direct biophotolysis) or organic compounds (indirect biophotolysis) are transferred to ferredoxin and then [FeFe]-hydrogenase resulting in H₂ production²⁶. By contrast, dark fermentative metabolism involves the glycolytic breakdown of organic compounds (e.g. intracellularly stored starch). The resulting pyruvate is then oxidized to acetyl-CoA by pyruvate ferredoxin oxidoreductase (PFR) resulting in carbon dioxide²⁵. Acetyl-CoA is then converted to stored lipids. The ferredoxin reduced by PFR is in turn reoxidized by [FeFe]-hydrogenase resulting in H₂ production²⁷. Photobiological H₂ production can be excluded as these pathways require light yet all experiments were conducted in darkness. Therefore, the most likely pathway to be responsible for the observed H₂ production is dark fermentative metabolism. The transfer of electrons from the reduced form of ferredoxin to hydrogenase, which is required for dark fermentation to proceed, can be effectively inhibited by low concentrations of metronidazole²⁸. Consistent with this H₂ production pathway, we observed administration of 5 mg/L metronidazole effectively inhibited H₂ production compared to a control treatment (Fig 2b).

We subsequently investigated the fate of the organic end products produced through dark fermentation. Dark fermentation in microalgae results in the production of a wide variety of organic end products in addition to H₂ and CO₂ depending on the microalgal species, pathway and environmental conditions^{12,29}. For example, *Chlamydomonas* excrete acetate, ethanol, and formate or glycerol at ratios that vary depending on the species³⁰. Additionally, some algae do not release fermentative products from the cell at all and instead they accumulate them intracellularly. For instance, Inui et al (1982)³¹ have found that *Euglena gracilis* generates large concentrations of wax esters which are stored in the cytosol³² that are reoxidized to generate ATP upon return to oxic conditions. We were unable to detect any alcohols or volatile fatty acids in the column effluent using solid phase micro extraction (SPME) followed by GC/MS analysis with a detection limit of <1 μM, suggesting that that fermentation products are predominantly stored intracellularly. We therefore performed metabolomic analysis of sediment collected from dark anoxic FTRs under H₂ production to detect possible storage products. This showed a 3 fold increase in phosphoglycerolipids and ceramides and a 5 fold increase in oleate (Fig 2c) as compared with oxic conditions. This is consistent with the synthesis of lipids from the fermentation product acetyl-CoA as previously documented for green algae (Fig 3)²⁵. Reactions 1 and 2 indicate possible stoichiometries for the breakdown of glucose to produce oleic acid and other fermentative products and are spontaneous under standard conditions. Under non-standard conditions, both reactions remain spontaneous regardless of high partial pressures of H₂ and CO₂ (0.8 atm), however, reaction 2 becomes most favourable at pCO₂ and pH₂ < 0.3 atm (see Supplementary Information Figure S2).





Using a combination of reactions 1 and 2, a wide range of CO₂:H₂ production stoichiometries are possible. No H₂ production was observed until ~48 h after anoxia, suggesting a reaction analogous to 1 before a reaction analogous to 2 commenced or net H₂ consumption. Once net H₂ production commenced, it was produced at 30-50% of the rate of DIC production, however, we note that the gross H₂ production rate is most likely higher than this. By analogy with other sediment ecosystems, it is more likely that much of the H₂ produced is immediately recycled by respiratory hydrogenotrophic bacteria inhabiting the sediments³³. Microbial ecology studies have shown that there is an abundance of both aerobic and anaerobic bacteria in these sediments^{33,34,35} with phylotypes similar to known hydrogenotrophs^{26,34,35}. If we assume that denitrification was the dominant electron sink and is driven by hydrogenotrophy, with a 2H₂:NO₃⁻ stoichiometry, then the total H₂ production rates could be double the release measured here. It remains unclear why any release of H₂ occurs because bacteria normally rapidly consume it. We speculate that in highly dynamic sand environments, bacterial biomass is unable to accumulate and that there is a lag time of days to weeks before their growth allows them to utilize all the H₂ once the environment becomes more static. In support of this hypothesis, we observe that sands become highly sulfidic ~1 week after collection from the field.

Diatoms and chlorophytes isolated from the permeable sediments fermentatively produce H₂

To further substantiate that microalgae produce H₂, we isolated and cultured representatives of two of the most dominant microalgal genera from the study sites (see Supplementary Information, Table S2). Axenic cultures of five diatom species (all *Fragilariopsis* sp.) and a chlorophyte (*Pyramimonas* sp.) were isolated from Port Phillip Bay. Incubations under dark anoxic conditions confirmed that all six cultures rapidly produced H₂ resulting in concentrations of 800 ± 450 nM after 118 hours of anoxic incubation (Fig 2d). While it is well-established that green algae can fermentatively evolve H₂³⁶, this to our knowledge is the first observation of H₂ production by diatoms. It has previously been observed that such organisms harbor the genes required to fermentatively produce H₂¹², i.e. PFR and [FeFe]-hydrogenase, thereby supporting our observations. It has long been recognized that diatoms can survive for many weeks in darkness³⁷ and that they may do this through dissimilatory nitrate reduction in dark anoxic conditions³⁸. Whilst this mechanism is viable in relatively eutrophic habitats such as the Wadden Sea, which have high nitrate concentrations over the winter months, this mechanism is unlikely to be viable in relatively oligotrophic habitats such as Port Phillip Bay, where nitrate concentrations are very low in the water column (typically < 1 μM) and there is intense competition for the little nitrate that exists. We therefore propose that fermentation is the principle mechanism that these dominant organisms use to persist during anoxia.

Summary

The results presented here challenge the conventional formulation of anoxic metabolic pathways using the redox cascade in high energy permeable sediments^{39,40}. We demonstrated here that the previously-identified carbon mineralization pathways (e.g. nitrate respiration, sulfate and iron reduction) and organisms (i.e. respiratory bacteria) in permeable sediments do not account for DIC production during anoxia. Instead, dark fermentation mediated by microalgae may be the dominant metabolic pathway, resulting in H₂ release and DIC production. Given that light penetration is sufficient to support positive net benthic community production can occur over 33% of the coastal ocean⁴¹, this may be a globally important metabolic pathway. It is also plausible that the H₂ produced is recycled by aerobic and anaerobic respiratory bacteria, thereby shaping ecology and biogeochemistry within the temporally and spatially variable ecosystem of the permeable sediment. In light of these findings, we are presently investigating the molecular pathways of carbon mineralization and H₂ metabolism in this ecosystem. Further studies are also required in realistic flow settings such as *in situ* or in flumes to investigate the dynamics of H₂ cycling in this ecosystem.

Materials and Methods

Flow through reactor experiments

Flow through reactor experiments (FTRs) were packed using approximately the top 15 cm layer of sediment from Port Phillip Bay, Victoria, Australia and Kerteminde, Denmark as described in Table 1. The FTRs used were acrylic cylinders with a diameter of 4.6 cm and a length of 3 cm sediment. PVC caps were placed at either end of the cylinder, and were machined with grooves converging to a central outlet port overlaid with 0.1 mm nylon mesh to allow even plug flow through the column. Plug flow within these columns has been verified during breakthrough curve experiments performed by Evrard *et al*⁴² and Bourke *et al*⁴³. Freshly collected site water was pumped through the FTRs using a peristaltic pump located upstream of the FTR. Reservoirs were maintained in oxic/anoxic states by continuous purging with air or argon respectively. The system was confirmed to have negligible leak rate of oxygen by running deoxygenated water through the system, which was then observed to have a concentration of <1 μM at the outlet. For H₂, a loss of 3.6% was observed when a solution containing 50 μmol L⁻¹ H₂ was pumped through the FTR set up. Water samples at the column outlet were collected by directly connecting glass syringes to the outlet tubing and ensuring no bubbles were present. Reaction rates were calculated based on the difference between the relevant solute concentration in the reservoir and the outlet of the column, the reactor volume and the flow rate through the reaction.

Solute and gas measurement

Oxygen was monitored at the inlet and outlet of the columns using Pyroscience Firesting flow through dissolved oxygen sensors. Denitrification rates were calculated using the isotope pairing technique⁴⁴ with the addition of 50 μM ¹⁵NO₃⁻ and we report total denitrification rates here (denitrification of ¹⁴NO₃⁻(D₁₄) and ¹⁵NO₃⁻(D₁₅)). Samples for analysis of ¹⁵N-N₂ were transferred from glass syringes into 12 mL Exetainers (Labco, High Wycombe, UK) and preserved with 250 μL of 50% w/v ZnCl₂. Samples for dissolved

inorganic carbon were sampled into 3 mL Exetainers and preserved with 30 μL of 6% HgCl_2 before analysis using flow injection analysis⁴⁵ with a precision $<1\%$. H_2 analyses were performed using a calibrated Unisense H_2 -100 sensor (Unisense A/S, Aarhus, Denmark) fitted with a glass flow through cell connected directly to the column outlet. Nitrate and nitrite concentrations were determined using a Lachat Quickchem 8000 flow injection analyser fitted with a spectrophotometric detector. A UV-Visible spectrophotometer (GBC) was used to determine iron and sulfide concentrations in FTR effluent following the Ferrozine^{46,47} and Fonselius⁴⁸ methods, respectively. Iron and sulfide samples were filtered using MicroAnalytix 0.2 μm cellulose-acetate filters and were preserved using 0.5 mL of Ferrozine and 100 μL of Zn acetate per mL of sample, respectively. Alkalinity production was quantified using a modified Gran titration⁴⁹. Following the addition of 100 μL aliquots of 0.01 mol L^{-1} HCl, changes in pH were recorded using an NBS buffer calibrated pH electrode attached to a portable HACH HQ40d meter. Chlorophyll *a* content was analysed using a UV-Visible spectrophotometer (GBC), following a methanol extraction step⁵⁰. Sediment organic carbon and isotope ratios were analysed using a Sercon 20-22 Isotope-Ratio Mass Spectrometer. Methane samples were preserved using 100 μL 50% w/v ZnCl_2 and given a 4 mL He headspace, prior to analysis. Methane concentration in samples was determined using a Varian 3700 Gas Chromatograph with a C-18 Poracil column equipped with a flame ionization detector. Intracellular nitrate pools were measured on freshly collected samples before and after exposure to nitrate concentrations of 50 μM . Samples were extracted according to Stief, et al. 17 before analysis for nitrate, as described previously.

Metabolome analysis

For metabolome analysis, cells were lysed and metabolites were extracted from sediments in the FTRs in a methanol:chloroform mixture (1:2, v:v; -20C°) for 30 min under sonication. The metabolites in the supernatants were analysed by GC-QTOF-MS and LC-QTOF-MS (both Agilent Technologies) following Godzien, et al. 51 and Kind, et al. 52 with slight modifications. Volatile fatty acid concentration in FTR effluent was determined using SPME GC-MS. A HP-5MS non polar column (Agilent Technologies, Mount Waverley, Australia) of dimensions 30 m x 0.25 mm ID x 0.25 μm film thickness was used for separation in conjunction with splitless injection mode and H_2 carrier gas. The method was optimized by exposing Carboxen/Polydimethylsiloxane SPME fibre to 10 mL of sample seawater headspace at 50C° for 60 min with 2g NaCl and acid addition prior to injection.

Microbiological analysis

For microalgal counts, sediment and culture samples were preserved with Lugols iodine solution and identified and quantified at MicroAlgal Services, (Ormond, Victoria, Australia) using a Zeiss Standard compound microscope equipped with Phase Contrast Optics with up to 400x magnification used in a Sedgewick-Rafter counting chamber. The identification of MPB present in the sediment samples was carried out using reference material from Grethe 53. Microalgae were isolated from sediment collected at the study site (but not used for flow through reactor experiments) and grown in F/2 medium under continuous illumination at 60 $\mu\text{mol photons m}^{-2} \text{s}^{-1}$ at a temperature of 18C° . To ensure no bacterial growth, the cultures were treated with a dilute antibiotic cocktail containing ampicillin, streptomycin and

tetracycline with final concentrations of 40, 20 and 8 mg L⁻¹, respectively. Cultures were incubated in 3 mL gastight exetainers under dark anoxic conditions and supernatant H₂ concentrations were determined using the H₂-100 sensor.

Data Availability

The data that supports the findings of this study are available from the corresponding authors upon request.

Supplementary Material

Refer to Web version on PubMed Central for supplementary material.

Acknowledgments

This work was supported by the Australian Research Council grant DP1096457 awarded to PLMC and RNG. RNG was additionally supported by Danish Council for independent Research, Natural Sciences, FNU, (0602-02276B) and the European Research Council through an Advanced Grant (ERC-2010-AdG20100224). The data reported in this paper can be made available by contacting the primary author. We thank Jack Middelburg and 3 anonymous reviewers for thoughtful comments on this work.

References

1. MacIntyre HL, Geider RJ, Miller DC. Microphytobenthos: The ecological role of the "secret garden" of unvegetated, shallow-water marine habitats 1. Distribution, abundance and primary production. *Estuaries*. 1996; 19:186–201.
2. Jahnke RA, Nelson JR, Marinelli RL, Eckman JE. Benthic flux of biogenic elements on the Southeastern US continental shelf: influence of pore water advective transport and benthic microalgae. *Cont Shelf Res*. 2000; 20:109–127.
3. de Jonge VN. Fluctuations in the organic carbon to chlorophyll *a* ratios for estuarine benthic diatom populations. *Marine Ecology Progress Series*. 1980; 2:345–353.
4. Light, B.; B, J. Distribution and primary productivity of microphytobenthos in Port Phillip Bay. CSIRO Institute of Natural Resources and Environment; 1998. p. 67
5. Rusch A, Forster S, Huettel M. Bacteria, diatoms and detritus in an intertidal sandflat subject to advective transport across the water-sediment interface. *Biogeochemistry*. 2001; 55:1–27.
6. Evrard V, Cook PLM, Veuger B, Huettel M, Middelburg JJ. Tracing incorporation and pathways of carbon and nitrogen in microbial communities of photic subtidal sands. *Aquat Microb Ecol*. 2008; 53:257–269.
7. Valdemarsen T, Kristensen E. Degradation of dissolved organic monomers and short-chain fatty acids in sandy marine sediment by fermentation and sulfate reduction. *Geochim Cosmochim Acta*. 2010; 74:1593–1605.
8. Boudreau BP, et al. Permeable marine sediments: Overturning an old paradigm. *EOS, Trans Am Geophys Union*. 2001; 82:133–136.
9. Veuger B, van Oevelen D. Long-term pigment dynamics and diatom survival in dark sediment. *Limnol Oceanogr*. 2011; 56:1065–1074.
10. Kamp A, de Beer D, Nitsch JL, Lavik G, Stief P. Diatoms respire nitrate to survive dark and anoxic conditions. *Proc Nat Acad Sci USA*. 2011; 108:5649–5654. [PubMed: 21402908]
11. Zhang LP, Happe T, Melis A. Biochemical and morphological characterization of sulfur-deprived and H₂-producing *Chlamydomonas reinhardtii* (green alga). *Planta*. 2002; 214:552–561. [PubMed: 11925039]
12. Atteia A, van Lis R, Tielens AGM, Martin WF. Anaerobic energy metabolism in unicellular photosynthetic eukaryotes. *Biochimica Et Biophysica Acta-Bioenergetics*. 2013; 1827:210–223.

13. Evrard V, Glud RN, Cook PLM. The kinetics of denitrification in permeable sediments. *Biogeochemistry*. 2013; 113:563–572.
14. Marchant HK, et al. Coupled nitrification-denitrification leads to extensive N loss in subtidal permeable sediments. *Limnol Oceanogr*. 2016; 61:1033–1048.
15. Pallud C, Meile C, Laverman AM, Abell J, Van Cappellen P. The use of flow-through sediment reactors in biogeochemical kinetics: Methodology and examples of applications. *Mar Chem*. 2007; 106:256–271.
16. Cook PLM, Wenzhofer F, Glud RN, Janssen F, Huettel M. Benthic solute exchange and carbon mineralization in two shallow subtidal sandy sediments: Effect of advective pore-water exchange. *Limnol Oceanogr*. 2007; 52:1943–1963.
17. Stief P, Kamp A, de Beer D. Role of Diatoms in the Spatial-Temporal Distribution of Intracellular Nitrate in Intertidal Sediment. *Plos One*. 2013; 8
18. Luthzhoft HCH, Halling-Sorensen B, Jorgensen SE. Algal toxicity of antibacterial agents applied in Danish fish farming. *Arch Environ Contam Toxicol*. 1999; 36:1–6. [PubMed: 9828255]
19. Hoehler TM, Albert DB, Alperin MJ, Martens CS. Acetogenesis from CO₂ in an anoxic marine sediment. *Limnol Oceanogr*. 1999; 44:662–667.
20. Finke N, Jorgensen BB. Response of fermentation and sulfate reduction to experimental temperature changes in temperate and Arctic marine sediments. *ISME J*. 2008; 2:815–829. [PubMed: 18309360]
21. Halling-Sorensen B, Luthzhoft HCH, Andersen HR, Ingerslev F. Environmental risk assessment of antibiotics: comparison of mecillinam, trimethoprim and ciprofloxacin. *J Antimicrob Chemother*. 2000; 46:53–58.
22. Robinson AA, Belden JB, Lydy MJ. Toxicity of fluoroquinolone antibiotics to aquatic organisms. *Environ Toxicol Chem*. 2005; 24:423–430. [PubMed: 15720004]
23. Kummerer K, Al-Ahmad A, Mersch-Sundermann V. Biodegradability of some antibiotics, elimination of the genotoxicity and affection of wastewater bacteria in a simple test. *Chemosphere*. 2000; 40:701–710. [PubMed: 10705547]
24. Martins N, et al. Ecotoxicological effects of ciprofloxacin on freshwater species: data integration and derivation of toxicity thresholds for risk assessment. *Ecotoxicology*. 2012; 21:1167–1176. [PubMed: 22373897]
25. Catalanotti C, Yang W, Posewitz MC, Grossman AR. Fermentation metabolism and its evolution in algae. *Front Plant Sci*. 2013; 4:150. [PubMed: 23734158]
26. Greening C, et al. Genomic and metagenomic surveys of hydrogenase distribution indicate H-2 is a widely utilised energy source for microbial growth and survival. *Isme Journal*. 2016; 10:761–777. [PubMed: 26405831]
27. Dubini A, Mus F, Seibert M, Grossman AR, Posewitz MC. Flexibility in anaerobic metabolism as revealed in a mutant of *Chlamydomonas reinhardtii* lacking hydrogenase activity. *J Biol Chem*. 2009; 284:7201–7213. [PubMed: 19117946]
28. Lloyd D, Kristensen B. Metronidazole inhibition of hydrogen production *in vivo* in drug sensitive and resistant strains of *Trichomonas vaginalis*. *J Gen Microbiol*. 1985; 131:849–853.
29. Ohta S, Miyamoto K, Miura Y. Hydrogen evolution as a consumption mode of reducing equivalents in green algal fermentation. *Plant Physiol*. 1987; 83:1022–1026. [PubMed: 16665317]
30. Mus F, Dubini A, Seibert M, Posewitz MC, Grossman AR. Anaerobic acclimation in *Chlamydomonas reinhardtii* - Anoxic gene expression, hydrogenase induction, and metabolic pathways. *J Biol Chem*. 2007; 282:25475–25486. [PubMed: 17565990]
31. Inui H, Miyatake K, Nakano Y, Kitaoka S. Wax ester fermentation in *Euglena gracilis*. *FEBS Lett*. 1982; 150:89–93.
32. Tucci S, Vacula R, Krajcovic J, Proksch P, Martin W. Variability of Wax Ester Fermentation in Natural and Bleached *Euglena gracilis* Strains in Response to Oxygen and the Elongase Inhibitor Flufenacet. *J Eukaryot Microbiol*. 2010; 57:63–69. [PubMed: 20015184]
33. Schwartz, E.; Fritsch, J.; Friedrich, B. *The Prokaryotes: Prokaryotic Physiology and Biochemistry*. Rosenberg, Eugene, et al., editors. Springer; Berlin Heidelberg: 2013. p. 119-199.

34. Hirst AD, Goldberg DM. Application of new ultra-micro spectrophotometric determination for serum hydroxybutyrate dehydrogenase activity to diagnosis of myocardial infarction. *Brit Heart J*. 1970; 32:114–&. [PubMed: 5417839]
35. Dykema S, et al. Ubiquitous Gammaproteobacteria dominate dark carbon fixation in coastal sediments. *Isme Journal*. 2016; 10:1939–1953. [PubMed: 26872043]
36. Melis A. Photosynthetic H₂ metabolism in *Chlamydomonas reinhardtii* (unicellular green algae). *Planta*. 2007; 226:1075–1086. [PubMed: 17721788]
37. Dupreez DR, Bate GC. Dark survival of the surf diatom *Anaulus australis* drebbs et schulz. *Bot Mar*. 1992; 35:315–319.
38. Heisterkamp IM, Kamp A, Schramm AT, de Beer D, Stief P. Indirect control of the intracellular nitrate pool of intertidal sediment by the polychaete *Hediste diversicolor*. *Mar Ecol Prog Ser*. 2012; 445:181–192.
39. Canfield DE, et al. Pathways of organic carbon oxidation in 3 continental margin sediments. *Mar Geol*. 1993; 113:27–40. [PubMed: 11539842]
40. Canfield DE, Thamdrup B, Hansen JW. The anaerobic degradation of organic matter in danish coastal sediments- iron reduction, manganese reduction and sulfate reduction. *Geochim Cosmochim Acta*. 1993; 57:3867–3883. [PubMed: 11537734]
41. Gattuso JP, et al. Light availability in the coastal ocean: impact on the distribution of benthic photosynthetic organisms and their contribution to primary production. *Biogeosciences*. 2006; 3:489–513.
42. Evrard V, Glud RN, Cook PLM. The kinetics of denitrification in permeable sediments. *Biogeochemistry*. 2012; 113:563–572.
43. Bourke M, Kessler A, Cook P. Influence of buried *Ulva lactuca* on denitrification in permeable sediments. *Mar Ecol Prog Ser*. 2014; 498:85–94.
44. Nielsen LP. Denitrification in sediment determined from nitrogen isotope pairing. *FEMS Microbiol Ecol*. 1992; 86:357–362.
45. Oshima M, et al. Highly sensitive determination method for total carbonate in water samples by flow injection analysis coupled with gas-diffusion separation. *Analyt Sci*. 2001; 17:1285–1290. [PubMed: 11759510]
46. Stookey LL. Ferrozine- A new spectrophotometric reagent for iron. *Anal Chem*. 1970; 42:779–&.
47. Viollier E, Inglett PW, Hunter K, Roychoudhury AN, Van Cappellen P. The ferrozine method revisited: Fe(II)/Fe(III) determination in natural waters. *Appl Geochem*. 2000; 15:785–790.
48. Fonselius, SH. Methods of seawater analysis. Grasshoff, K., editor. Springer-Verlag; Chemie: 2007. p. 91-100.
49. Anderson, LG.; T, DR.; Wedborg, M.; Dyrssen, D. Ch. Determination of total alkalinity and total dissolved inorganic carbon. Methods of seawater analysis. Kremling, K.; Grasshoff, K.; Ehrhardt, M., editors. Springer-Verlag; 2007. p. 127-148.
50. Jeffrey SW, Humphrey GF. New spectrophotometric equations for determining chlorophylls *a*, *b*, *c1* and *c2* in higher plants, algae and natural phytoplankton. *Biochem Physiol PFL*. 1975; 167:191–194.
51. Godzien J, et al. In-vial dual extraction liquid chromatography coupled to mass spectrometry applied to streptozotocin-treated diabetic rats. Tips and pitfalls of the method. *J Chromatogr A*. 2013; 1304:52–60. [PubMed: 23871561]
52. Kind T, et al. FiehnLib: Mass Spectral and Retention Index Libraries for Metabolomics Based on Quadrupole and Time-of-Flight Gas Chromatography/Mass Spectrometry. *Anal Chem*. 2009; 81:10038–10048. [PubMed: 19928838]
53. Grethe, S.; E, E. Identifying Marine Phytoplankton. Tomas, CK., editor. Elsevier Inc; 1997. p. 5-385.

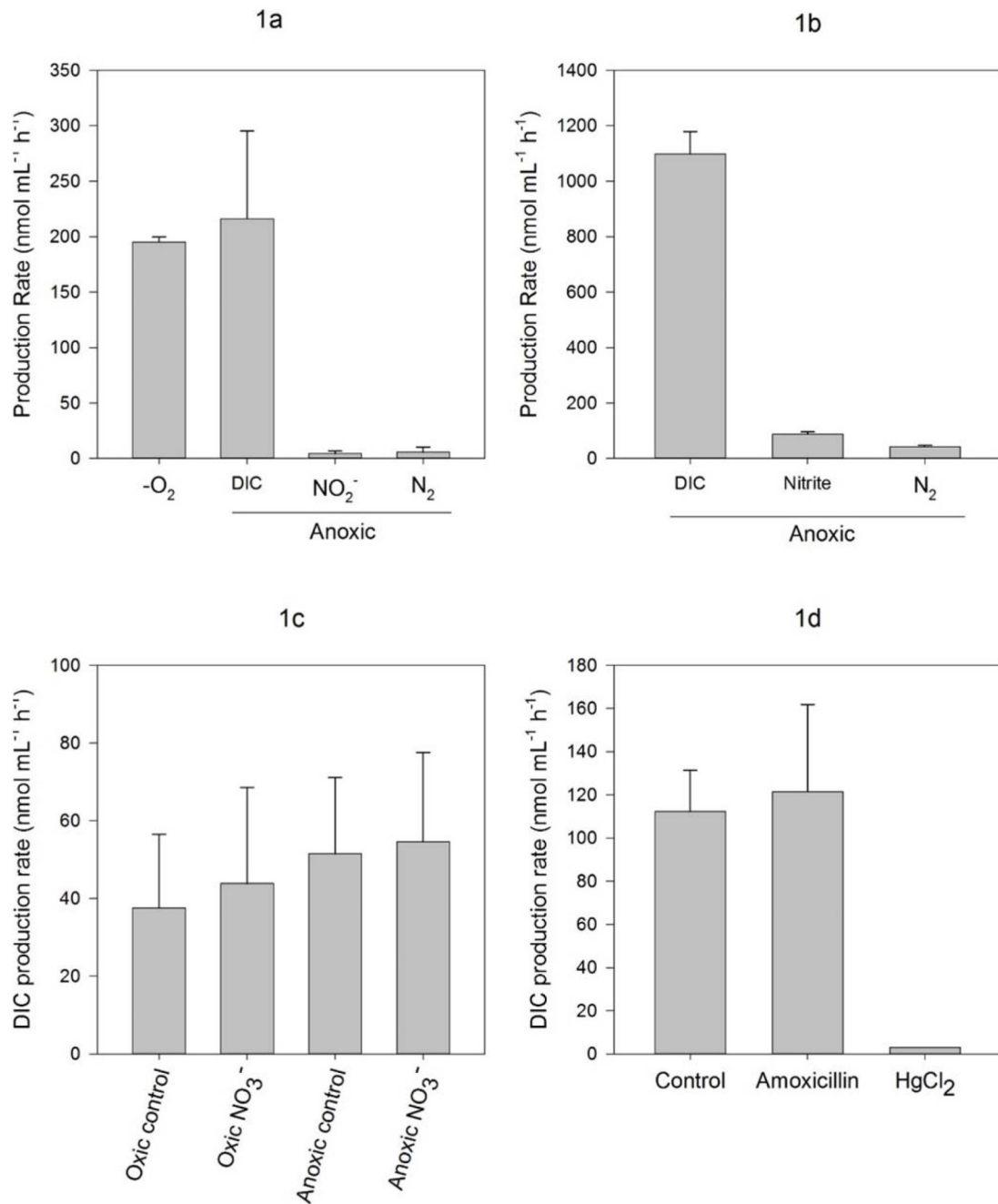


Figure 1.

Metabolism measured in FTR experiments. Sediments collected from Port Phillip Bay, Australia (a,c,d) and Kerteminde, Denmark (b). (a), (b) Oxygen consumption, dissolved inorganic carbon (DIC), nitrite and dinitrogen (as N) production in experiments switched anoxic after O₂ consumption was measured n=4. c) DIC production rates under oxic and anoxic conditions and in the presence and absence of nitrate, n=3 for each treatment. d) DIC production under anoxic conditions: control (n=2), in presence of 50 mg L⁻¹ amoxicillin (n=2) and 2 mmol L⁻¹ HgCl₂ (n=1). All error bars are standard deviation.

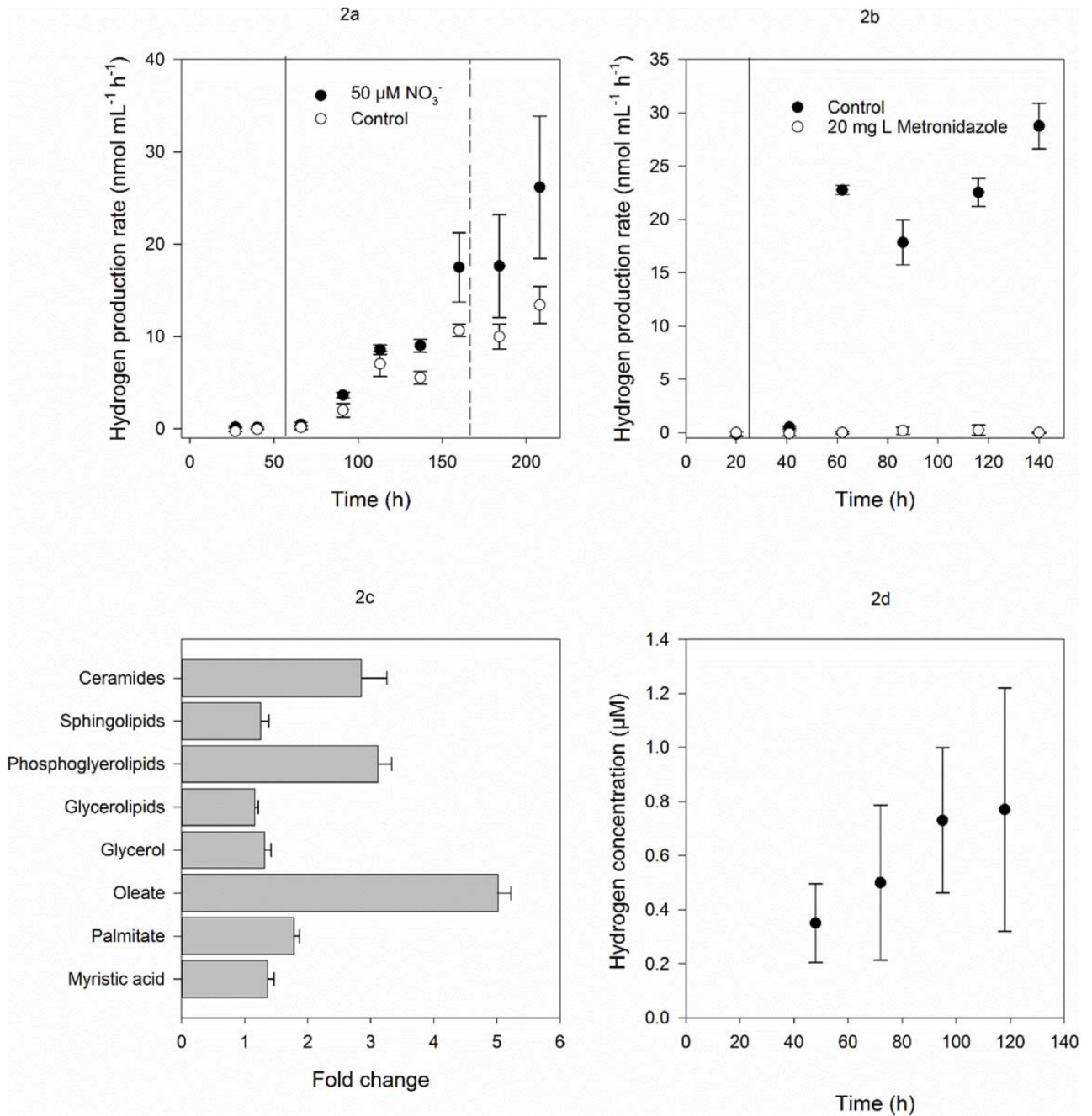


Figure 2.

H₂ and metabolite production in permeable sediments from flow through reactor experiments (a-c) and cultures (d). (a) H₂ production in the presence and absence of 50 μM nitrate. The solid line and broken lines represent a change from oxic to anoxic conditions and the addition of 150 μmol L⁻¹ ciprofloxacin respectively, n=3. (b) H₂ production in a control and 20 mg L⁻¹ metronidazole, n=3. (c) The relative concentration of metabolites during H₂ production compared to oxic conditions, n=3. (d) H₂ production in cultures of five

diatom species and a chlorophyte incubated anoxically in the dark, n=6. Error bars represent standard deviations.

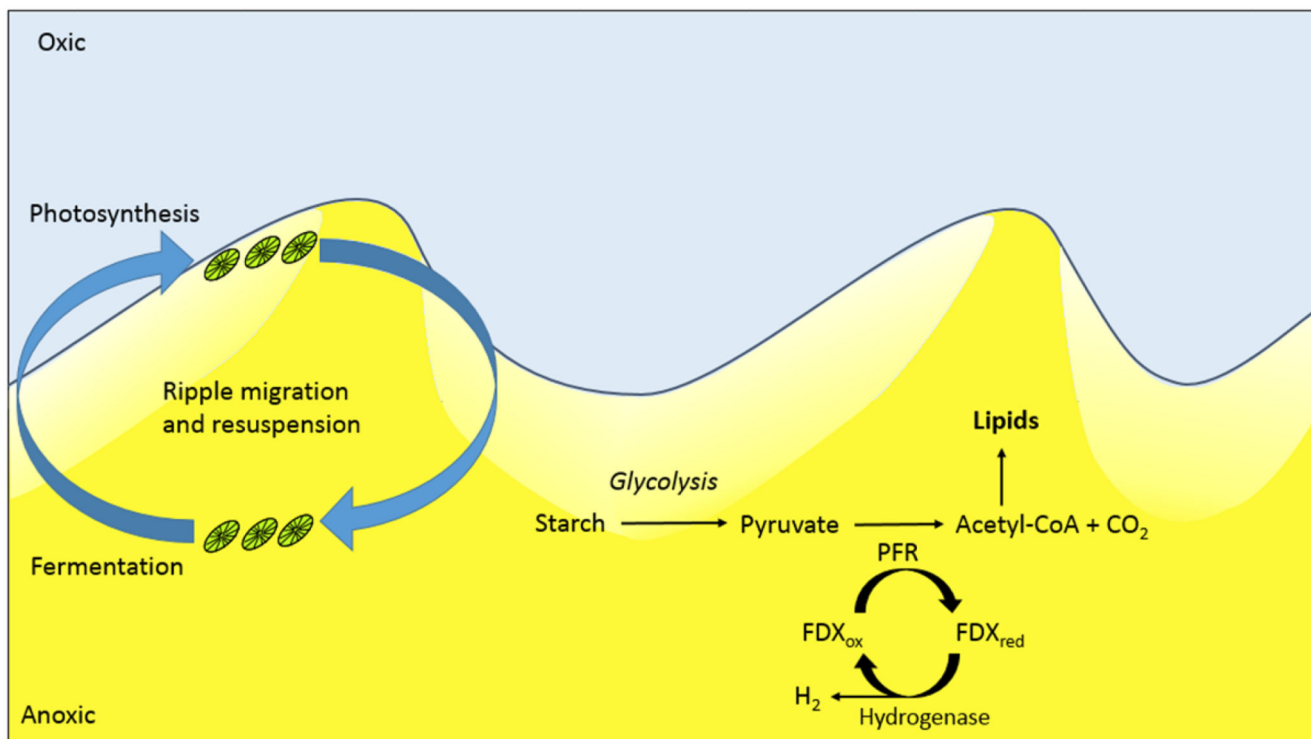


Figure 3.

Conceptual model of benthic algal metabolism in sand sediments. In this energetic environment, ripple migration and sediment resuspension regularly move algal cells many centimetres into the sediment where it is dark and anoxic. Under these conditions, microalgae undertake dark fermentation associated with high rates of H₂ and lipid production²⁵. Enzyme designations are pyruvate ferredoxin oxidoreductase (PFR) and ferredoxin (FDX). Lightly shaded areas represent declining oxygen concentration within the sediment. Yellow shaded area represents anoxic permeable sediment.

Table 1

List of experiments performed, location, date of sediment collection and products measured. Coordinates for the sites are 55°27'20.65", 10°39'56.14"E for Kerteminde and 37°51'8.73"S, 144°57'27.07"E for Port Phillip Bay. Note sampling was carried out in all seasons and so temporal variability explains the variability of DIC production rates presented in Figure 1.

Figure	Location	Date	Flow Rate (mL min ⁻¹)	Products measured.
1a	Port Phillip Bay , Victoria, Australia	16/09/2014	1.0	DIC, ²⁸ N ₂ , ²⁹ N ₂ , ³⁰ N ₂ , Nitrite, Iron and Sulfide.
1b	Kerteminde, Denmark.	7/11/2012	0.38	DIC, ²⁸ N ₂ , ²⁹ N ₂ , ³⁰ N ₂ , Nitrite.
1c, 2a, 2c	Port Phillip Bay , Victoria, Australia	15/08/2015	0.39	DIC, Dissolved H ₂ , metabolomic analysis.
1d	Port Phillip Bay , Victoria, Australia	6/03/2015	0.72	DIC, ²⁸ N ₂ , ²⁹ N ₂ , ³⁰ N ₂
-	Port Phillip Bay , Victoria, Australia	23/01/2014	-	Intracellular nitrate accumulation
2b	Port Phillip Bay , Victoria, Australia	31/10/2015	0.87	Dissolved H ₂
2d	Port Phillip Bay , Victoria, Australia *	12/12/2015		Dissolved H ₂

* Sediment collected in this instance was used to grow algal cultures that are presented in Figure 2d.